Prabu Moni, Amanda Deschamps, Daniel Schumacher, Kurosch Rezwan, Michaela Wilhelm

A new silicon oxycarbide based gas diffusion layer for zinc-air batteries

Prabu Moni, Amanda Deschamps, Daniel Schumacher, Kurosch Rezwan, Michaela Wilhelm,
A new silicon oxycarbide based gas diffusion layer for zinc-air batteries,
Journal of Colloid and Interface Science, Volume 577, 2020, Pages 494-502, ISSN 0021-9797,
https://doi.org/10.1016/j.jcis.2020.05.041

A new silicon oxycarbide based gas diffusion layer for zinc-air batteries

Prabu Moni [a,b], Amanda Deschamps [a,c], Daniel Schumacher [a], Kurosch Rezwan [a,d], Michaela Wilhelm [a,*]

[a] University of Bremen, Advanced Ceramics, Am Biologischen Garten 2, IW3, 28359 Bremen, Germany
[b] CSIR-Central Electrochemical Research Institute-Madras Unit, CSIR Madras Complex, Taramani, Chennai 600 113, India
[c] Department of Materials Engineering, Federal University of Santa Catarina (UFSC), 88040-900 Florianopolis, SC, Brazil
[d] University of Bremen, MAPEX Center for Materials and Processes, Bibliothekstraße 1, 28359 Bremen, Germany

HIGHLIGHTS

- A new ceramic gas diffusion layer has been prepared via polymer derived ceramics.
- 390 μm thick and 55% porous GDL is developed with the help of freeze tape casting.
- GDL shows a bilayer with a thin denser layer followed by sponge-like backing layer.
- The ceramic electrode shows the excellent performance in ZAB by breathing open air.
- Sponge-like GDL facilitates the oxygen exchange rate and offers better kinetics.

GRAPHICAL ABSTRACT

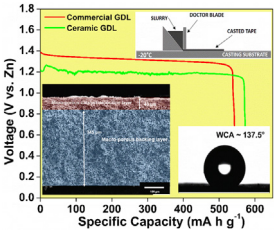

ABSTRACT

Rational material designs play a vital role in the gas diffusion layer (GDL) by increasing the oxygen diffusion rate and, consequently, facilitating a longer cycle life for metal-air batteries. In this work, a new porous conductive ceramic membrane has been developed as *a* cathodic GDL for zinc-air battery (ZAB). *The* bilayered structure *with* a thickness of 390 μm and an open porosity of 55% is derived from a preceramic precursor with the help of the freeze tape casting technique. The hydrophobic behaviour of the GDL is proved by the water contact angle of 137.5° after the coating of polytetrafluoroethylene (PTFE). The electrical conductivity of 5.59 * 10^{-3} S/cm is reached using graphite and MWCNT as filler materials. Tested in a ZAB system, the as-prepared GDL coated with commercial Pt-Ru/C catalyst shows an excellent cycle life over 200 cycles and complete discharge over 48 h by consuming oxygen from the atmosphere, which is comparable to commercial electrodes. The as-prepared electrode exhibits excellent ZAB performance due to the symmetric sponge-like structure, which facilitates the oxygen exchange rate and offers a short path for the oxygen ion/-electron kinetics. Thus, this work highlights the importance of a simple manufacturing process that significantly influences advanced ZAB enhancement.

Keywords:
Zinc-air battery
Gas diffusion layer
Porous membrane
Polymer-derived ceramics
Freeze tape casting

1. Introduction

Prolonging the cycle life of rechargeable ZABs has been a challenge, not only because of inefficient catalyst, zinc dissolution, and re-deposition but also due to the lack of satisfactory architecture of gas diffusion electrode (GDE) [1–4]. The GDE is generally

* Corresponding author.
E-mail address: mwilhelm@uni-bremen.de (M. Wilhelm).

manufactured by depositing the electrocatalyst on a carbon-based GDL, which controls the oxygen transport process [5]. The commercial GDL (SIGRACET® 39 BC) is a bilayered porous structure with (i) a macro-porous backing layer (carbon nanofiber) which is responsible for the transport, mechanical, thermal, and electrical properties; and (ii) a micro-porous structure (carbon allotropes) on which the electrocatalyst is deposited [5–9]. However, this commercial GDL has a complex manufacturing process [9]. Additionally, its pores are not aligned because an electrospinning process produces the backing layer, which causes low oxygen gas permeability and, consequently, affects the longer cycle life of ZAB [9–12].

Recently, silicon-based polymer-derived ceramics (PDC) had widely received enormous attention for applications such as energy storage/conversion, gas adsorption, and water separation/filtration [13–18]. Using a preceramic polymer enables the generation of a porous monolith with a tailorable pore size, pore morphology, surface characteristic, and electrical conductivity. All these properties are crucial requirements for GDL [19]. Since the GDL is a thin and flat membrane, tape casting is promising for its preparation with tailored thickness [20]. TCA e Silva et al. already prepared conductive SiOC anodes using tape casting. These anodes showed unusual characteristics in a microbial fuel cell system [19]. For GDLs, a further essential requirement is a multi-layered structure with aligned pores. The freeze-casting technique enables the production of 3D hierarchical porous ceramics with different shapes and geometries [21,22]. Recent results indicate that solution-based freeze casting is very vital for adjusting the pore morphology and surface functions of ceramic monoliths [23,24]. Hence, the combination of freeze casting with tape casting results in the freeze tape casting process to produce 3D hierarchical porous ceramic membranes. This technique is established for porous ceramic oxide materials, but there is no literature on freeze tape casting of PDCs [11,25]. In freeze tape casting, the choice of solvent, solid loading, fillers, and the solidification condition are critical to determining the structure and characteristics of the porous structure [23,26]. Further, the addition of conductive fillers (Graphite/-MWCNT) influences the rheological behaviour and the cross-linking degree of the polymer and alter the porosity, surface characteristics, mechanical stability, and electrical conductivity of GDL [5,27]. It is reported that the bilayered membrane, which is manufactured by freeze casting, could improve the oxygen flux when used as a support for solid oxide fuel cells [28]. Using freeze tape casting, Chen et al. prepared a hierarchically ordered porous ceramic $Sm_{0.5}Sr_{0.5}CoO_3$-$Gd_{0.1}Ce_{0.9}O_{2-\delta}$, which proved to be efficient cathode in low-temperature solid oxide fuel cells [25]. Schulze-Küppers et al. also studied the effect of tape-cast and freeze-dried supports ($Ba_{0.5}Sr_{0.5}(Co_{0.8}Fe_{0.2})_{0.97}Zr_{0.03}O_{3-\delta}$) on oxygen transport [11].

In this contribution, we have developed a new silicon-based GDL for ZAB with a less complicated process. Using tape casting, the polymer solution with controlled viscosity is cast onto a support using a doctor blade to control the thickness (between 325 and 450 μm). Immediate freezing of the tape leads to a porous bilayered membrane with a thin dense layer (~45 μm) in the upper part and a sponge-like backing layer (~345 μm). The open porosity (45–55%) is adjusted by changing the total solid loading of the polymer solution. To enhance the electrical conductivity, conductive fillers such as graphite and carbon nanotubes were added to the polymer solution. The superhydrophobic polytetrafluoroethylene (PTFE) coating was done on the GDL to improve the hydrophobicity (WCA > 120°). Electrical properties and ZAB performance were measured. Notably, a ceramic GDL based ZAB exhibits a long lifetime in battery condition due to better mass-transfer kinetics facilitated by the aligned bilayered structure with the improved oxygen exchange rate.

2. Experimental section

3D hierarchical porous ceramic GDLs were prepared by freeze tape casting using polysiloxane solutions. A commercial poly (methyl silsesquioxane) (Silres® MK, Wacker Chemie AG, Germany), 3-aminopropyltriethoxysilane (98%, abcr® APTES, GmbH, Germany), graphite (Gr)/-multi-walled carbon nanotubes (CNT) (Sigma Aldrich), and cyclohexane (Sigma Aldrich) were used as preceramic polymer, cross-linking agent, conductive fillers, and solvent, respectively. MK was dissolved in cyclohexane using a

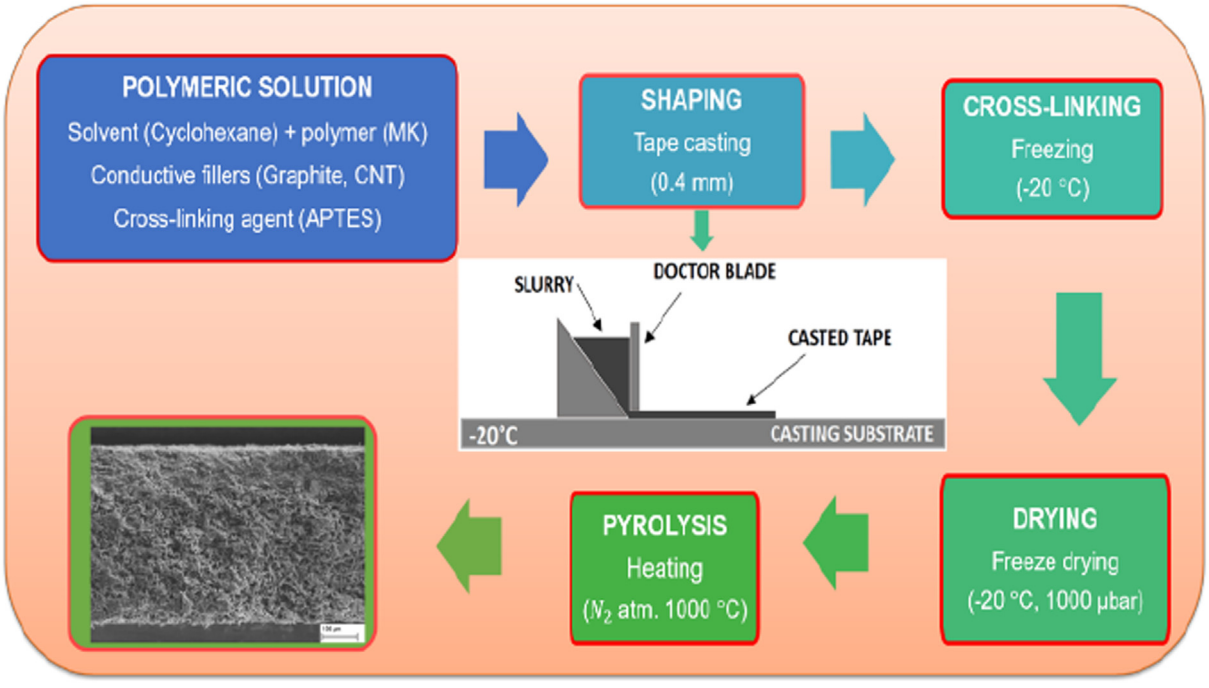

Scheme 1. Process scheme of ceramic gas-diffusion layer by freeze tape casting method.

magnetic stirrer at room temperature. Then, Gr/-CNT and APTES were added to the mixture. Subsequently, the solutions were tape cast with a thickness of ~0.4 mm on a pre-cooled (−20 °C) aluminum support using a doctor blade. For complete freezing and cross-linking, the cast membrane was transferred to a freezer at −20 °C for 72 h. Then the samples were freeze-dried at −20 °C for 72 h and a pressure of 1000 μbar. Finally, the green body was pyrolyzed at 1000 °C for 4 h in a nitrogen atmosphere to obtain a porous amorphous SiOC membrane. The preparation of a ceramic GDL by freeze tape casting is shown in Scheme 1. The GDLs were given the following nomenclature: MKxGry, where x is the total weight percent of solid loading, including polymer and conductive fillers, and y is the weight percent of conductive fillers within the solid fraction. Table S1 (Supporting Information) gives an outline of all samples with their compositions and Fig. S1 shows the photograph of prepared ceramic GDL.

The structural analysis of the ceramic GDL was obtained by using a Seifert XRD powder diffractometer (General Electric, USA). The morphology and the pore alignment were analyzed using SEM (Camscan Series 2, Obducat CamScan Ltd., and Zeiss supra 40, Gemini). The pore size distribution and total porosity were measured using Mercury Porosimetry (Pascal 140/440, POROTEC GmbH, Germany). Evaluation of nitrogen adsorption isotherms (Belsorp-Mini II, Bel Japan Inc), according to the Brunauer–Emmet t–Teller (BET) theory, resulted in the specific surface area. The apparent density was measured with the helium-pycnometer (ATC POROTEC GmbH, Germany). The bending strength of the GDL was characterized in a three-point bending test using a universal testing machine (UTM Zwick Z005, Germany) with the help of Weibull statistic distribution (details were reported in Fig. S2). Vapour adsorption measurements were performed using *n*-heptane and water as probe molecules. The surface wettability was evaluated by water contact angle experiments on a pendant drop tensiometer (DSA 100, DataPhysics, Germany). For a better understanding of ceramic GDL with commercial SIGRACET® 39 BC, the GDLs were undergone similar coating of polytetrafluoroethylene (PTFE), which is superhydrophobic, chemical resistant, and anti-corrosive [9]. The AC impedance spectroscopy was used to analyze the through-plane conductivity of the GDLs with an electrochemical workstation (IM6ex Zahner® Elektrik) in the frequency range from 10 mHz to 1 MHz and at an AC amplitude of 10 mV.

Finally, the ZAB testing was performed using a self-made battery setup. The commercial SIGRACET® 39 BC GDL acted as a reference and was compared with the ceramic GDLs. Commercial

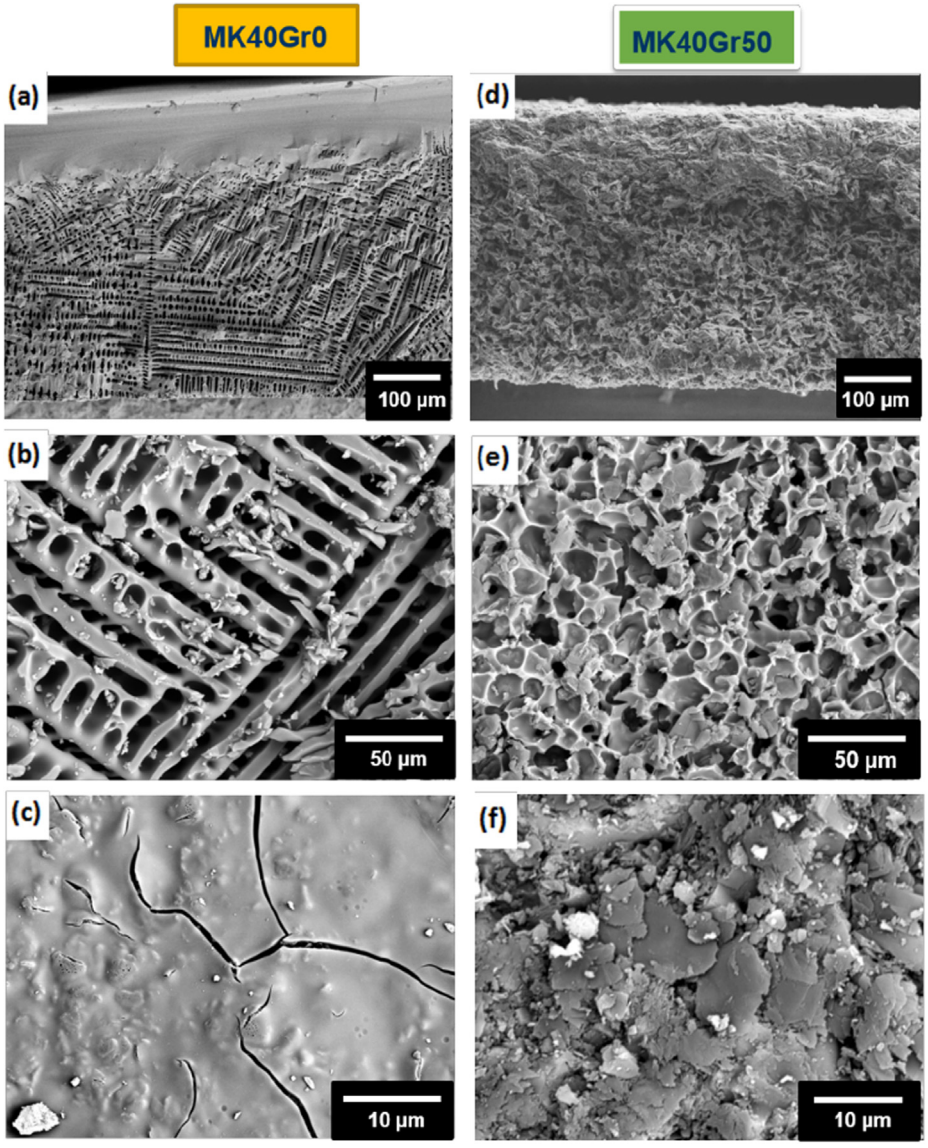

Fig. 1. Exemplary SEM images of the cross-sections (a, d), bottom surface (b, e), and top surface (c, f) of MK40Gr0 (left) and MK40Gr50 (right).

Pt-Ru/C with 40 wt% Pt and 20 wt% Ru on Vulcan XC-72R carbon was purchased from Quintech, Germany, as cathode electrocatalyst. The catalyst ink was prepared by mixing 3.5 mg of Pt-Ru/C in 300 μL of ethanol, 100 μL of deionized water, and 10 μL of 5 wt% Nafion. Then the air cathode was fabricated by applying the Pt-Ru/C catalyst ink on the ceramic GDL and the commercial GDL using hand brush coating technique with a catalyst mass of about 1 mg/cm^2. A ZAB, which was packed with polished zinc, a Whatman glass microfiber filter membranes wet by a 6 M KOH aqueous electrolyte and a catalyst-coated GDL. The ZAB experiments were performed using an electrochemical workstation (Biologic VMP3, France) at room temperature and atmospheric conditions. The specific capacity of ZAB was calculated based on the mass of zinc anode consumed for testing, and the cycling stability was tested for 10 min per cycle. The morphological stability of cycled GDLs was monitored after dismantling the ZAB and subjected to SEM analysis.

3. Results and discussion

In this tape casting process, the preceramic solution (MK + APTES) is mixed with cyclohexane in a controlled viscosity and is cast onto an aluminum substrate using a doctor blade assembly [19]. Later, directional freezing takes place by moving the casting bed into a freezer, where the solidification of the solvent started in a freezing direction by growing crystals. Then, during the freeze-drying, the completely frozen solvent was removed and thereby creates the pore morphology. By modifying the solid fraction, the total porosity obtained after solidification, sublimation, and pyrolysis treatment can be controlled [29]. When the total solid loading (MK and Gr/-CNT) was increased to 60 wt%, the suspension was too viscous to be tape cast. On the other hand, when the total solid loading was lower than 30 wt%, the viscosity was too small for tape casting. Hence, only samples with 40 wt% and 50 wt% of the total solid loading was further characterized [23,30]. The produced GDLs have an average thickness of ~390–450 μm and an area of 15 × 5 cm^2. The XRD pattern of ceramic GDL (MK40Gr0) pyrolyzed at 1000 °C shows the amorphous phase as shown in Fig. S3. Within this SiOC amorphous structure, the silica atom is tetrahedrally bonded to carbon and oxygen along with the disordered carbon phase [31].

Fig. 1 shows exemplary SEM images, including top, bottom, and cross-section area of ceramic GDL. The ceramic GDL without graphite (MK40Gr0) shows a bilayered geometry with a thick (~100 μm), dense layer in the upper part followed by a dendritic porous structure, which is characteristic for cyclohexane [29,32]. The dense layer is formed on the side, which is in contact with the atmosphere. Due to the high vapour pressure of cyclohexane, it quickly evaporates and leads to the formation of the dense layer [30]. With the addition of graphite particles into the ceramic matrix (MK40Gr50), the pore morphology of the backing layer changes to sponge-like (Fig. 1(d–f)). Schumacher et al. already reported that the addition of filler particles influences the pore morphology of ceramic membranes because the filler particles create small temperature variations and direct contact at the dendrite tips during the freezing, disrupting the growth of the solvent crystal [29]. The other samples show similar microstructures, e.g., MK40Gr50, MK50Gr50, and MK50Gr45CNT5, exhibit a bilayered geometry with a thin denser layer (~45 μm) and a sponge-like backing layer (~345 μm), as needed for ZAB application (Fig. 2) [33]. A similar type of microstructures was even observed at the top, bottom, and cross-section view of commercial SIGRACET® 39 BC GDL (Fig. S5). The top layer of bare ceramic GDL (MK50Gr0) shows a smooth surface, whereas, for graphite containing GDL (MK50Gr50), the rough surface was created by the graphite. Even a few MWCNTs were observed on the MWCNT-incorporated ceramic GDL (MK50Gr45CNT5) (Fig. S4). The influence of total solid loading and filler content on the pore size distribution and total open porosity were investigated by mercury intrusion porosimetry (Fig. 3). All GDLs shows the pore diameter varies in the range of 3–10 μm [34].

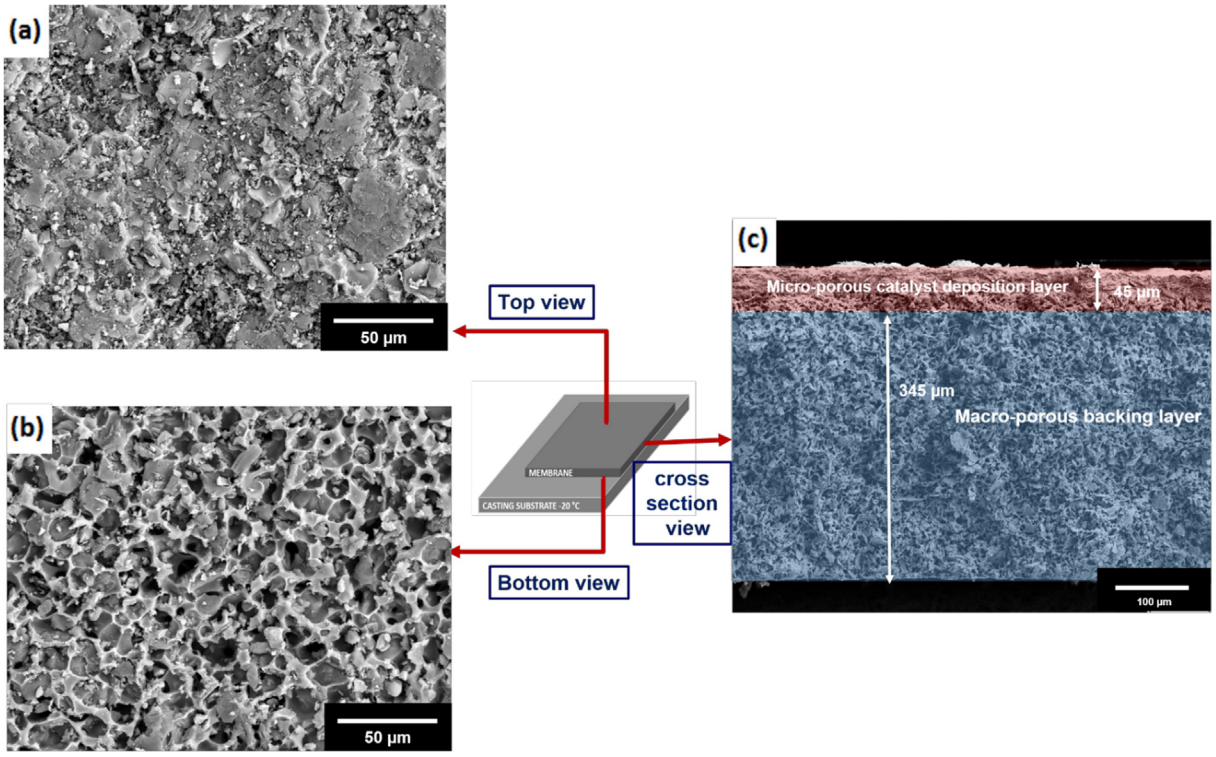

Fig. 2. SEM images of (a) top, (b) bottom and (c) cross-sectional view of MK50Gr45CNT5.

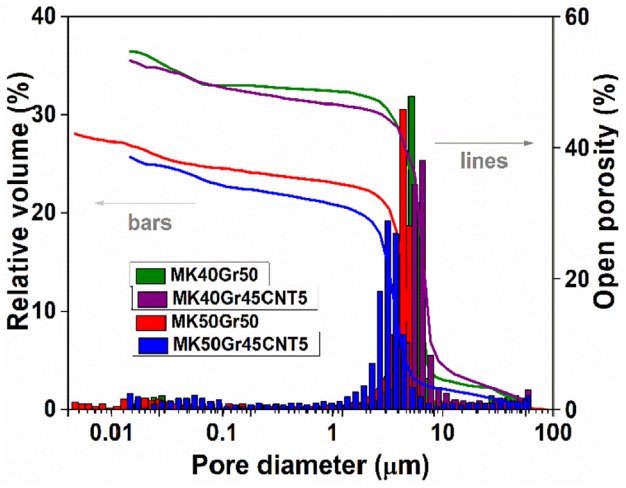

Fig. 3. Pore size distribution and open porosity of ceramic GDL obtained from Hg-intrusion porosimetry.

It has to be noted that though the pyrolysis temperature was not altered in this work, previous works show that the pyrolysis temperature has no significant impact on the macropore size of solution-based freeze cast SiOC monolith [29]. As the solid fraction is not composed of single particles but a continuous preceramic polymer, sintering as a mechanism for pore size reduction can be neglected. The GDLs with 40 wt% of total solid loading shows the highest open porosity of 55%, which is higher than the commercial GDL (SIGRACET® GDL 39 BC) with an open porosity of 50–52% [9]. When the total solid loading is increased to 50 wt%, the open porosity decreases to 40%, which is following the literature [35]. Since in freeze casting, the solvent acts as a template that forms the pore space after sublimation, the porosity mainly depends on the amount of solvent. A higher amount of solvent is equal to lower solid loading and consequently results in a higher porosity as it is observed when comparing the samples with 40 wt% and 50 wt% solid loading. However, GDLs with the same total solid loading and without graphite (MK40Gr0) show lower open porosity compared to graphite containing GDL (MK40Gr50) (Fig. S6). On the other hand, the specific surface area values increase with the addition of conductive fillers (Gr/-CNT) as an effect of interlayer packing of fillers, and also this filler influences the complete manufacturing process (Fig. S7) [36].

Fig. 4 shows the water contact angle (WCA) of ceramic GDLs. The Gr/-CNT containing GDLs shows a slightly more hydrophobic surface with a WCA of ~72.2° and 87.6° for MK40Gr50 and MK50Gr45CNT5, whereas the bare ceramic GDL (MK50Gr0) shows a hydrophilic surface with a WCA ~48.8° [19]. After coating PTFE, ceramic GDLs exhibit an increased hydrophobic surface with a WCA of ~120.2° and 137.5° for MK40Gr50 and MK50Gr45CNT5 respectively. These values are very close to the commercial GDL (SIGRACET® GDL 39 BC) with a WCA of ~144.1°. Hence, the ceramic GDLs coated with PTFE can be used for the ZAB application to avoid moisture uptake from the surrounding [37]. The three-point bending test was carried out to examine the influence of the open porosity on mechanical stability. Fig. 5 shows the Weibull distribution of the tensile strength. As expected, the sample with 40% of total solid loading (MK40Gr50) has a lower characteristic strength (σo = 12.8 MPa) and Weibull modulus (m = 8.8) when compared to MK50Gr45CNT5 (σo = 24 MPa, m = 9.5). Since the Weibull modulus is smaller, a larger dispersity of tensile strength for MK40Gr50 can be assumed [38]. These results confirm that the mechanical properties of ceramic GDLs highly depend on the total solid loading and type of fillers used. Additionally, the open porosity dominates the tensile strength [39]. Further, the two-probe AC impedance spectroscopy was performed to investigate the through-plane (TP) conductivity, which is an essential property of ZABs [6]. Fig. 6 shows the Arrhenius plot of ceramic GDL. The GDL without graphite (MK50Gr0) behaves like a semiconductor with a TP conductivity value of ~10^{-8} S/cm [19]. It can be noticed that the addition of Gr/-CNT improves the conductivity due to the formation of percolation paths provided by graphitic domains [19,40]. MK40Gr50 shows a TP conductivity of ~1.89 * 10^{-4} S/cm, which increases to ~2.67 * 10^{-3} S/cm for MK50Gr50. On the other hand, MK50Gr45CNT5 shows the highest conductivity, which is calculated to ~5.59 * 10^{-3} S/cm with an activation energy of 0.1 eV [41]. However, despite the excellent conductivity, ceramic GDLs have not shown a conductivity as high as the commercial GDL

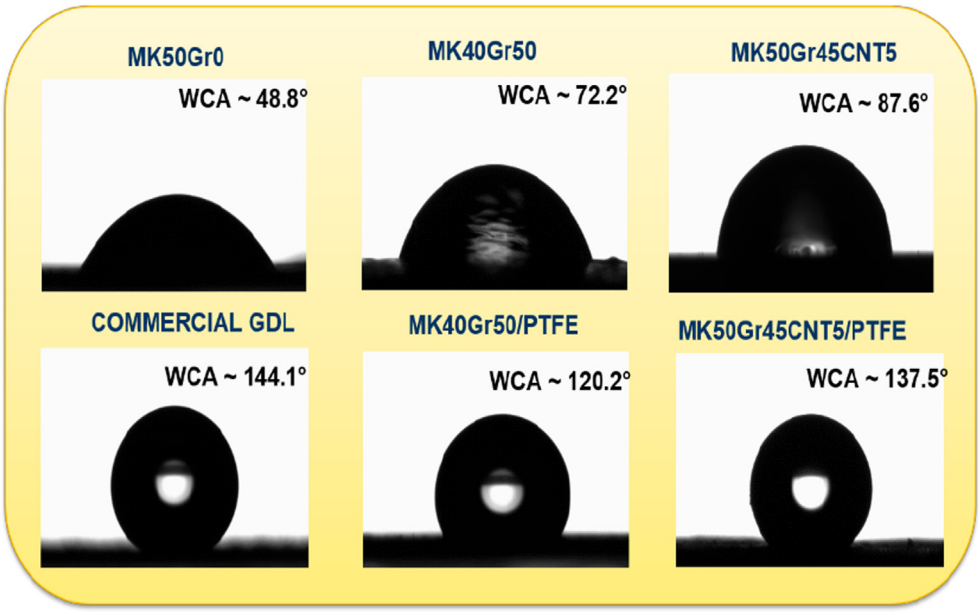

Fig. 4. Water contact angles of the ceramic GDLs at 25 °C.

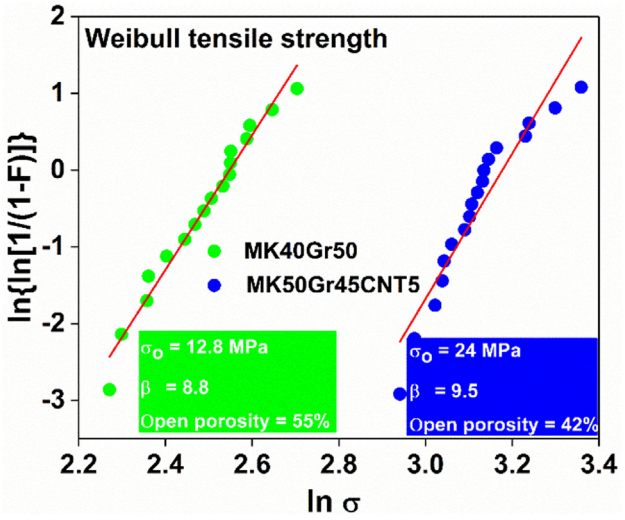

Fig. 5. Weibull tensile strength plot of ceramic GDLs.

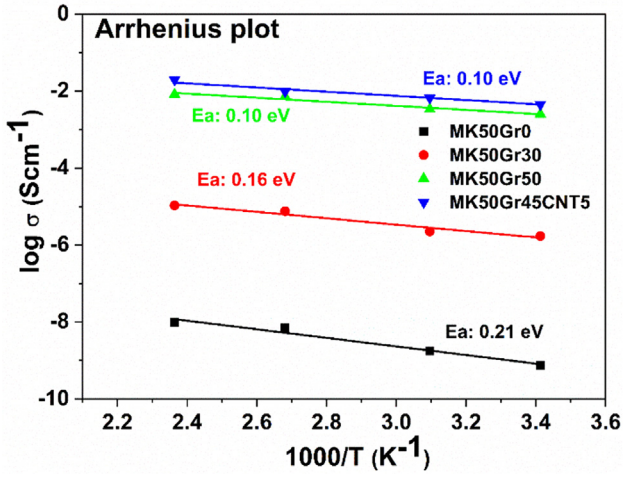

Fig. 6. Arrhenius plot of ceramic GDL measured by two-probe AC impedance spectroscopy.

(SIGRACET® GDL 39 BC; TP ~2 * 10^{-1} S/cm) and need further improvement for realistic performance.

Since the optimized ceramic membranes show all exciting features, which are required for air-breathing GDL, the ceramic membranes were further predesignated as a GDL for ZAB. Their performance was evaluated with the help of state of the art Pt-Ru/C catalyst. As a reference, the Pt-Ru/C catalyst was also coated on a commercial GDL (SIGRACET® GDL 39 BC), and the results were compared. In primary conditions, the ZABs were deeply discharged to 0.5 V at a current density of 3 mA/cm^2. As shown in Fig. 7a, b, the open-circuit voltage (OCV) of the commercial electrode is around ~1.33 V. In contrast, the highly conductive MK50Gr45CNT5/PTFE based electrode shows an OCV of ~1.2 V. The highly porous MK40Gr50/PTFE exhibits an OCV of ~1.1 V. The best ceramic GDL with 50 wt% carbon allotropes (MK50Gr45CNT5/PTFE) delivers a slightly lower OCV and working voltage since the conductivity is still less compared with commercial GDL, which is prepared with ~100 wt% of carbon allotropes. Despite their lower OCV and working potential, the ceramic GDL with higher porosity (MK40Gr50/PTFE) breathe in even longer and discharge over 48 h. Additionally, it delivers a much higher specific capacity of 625 mA h/g compared

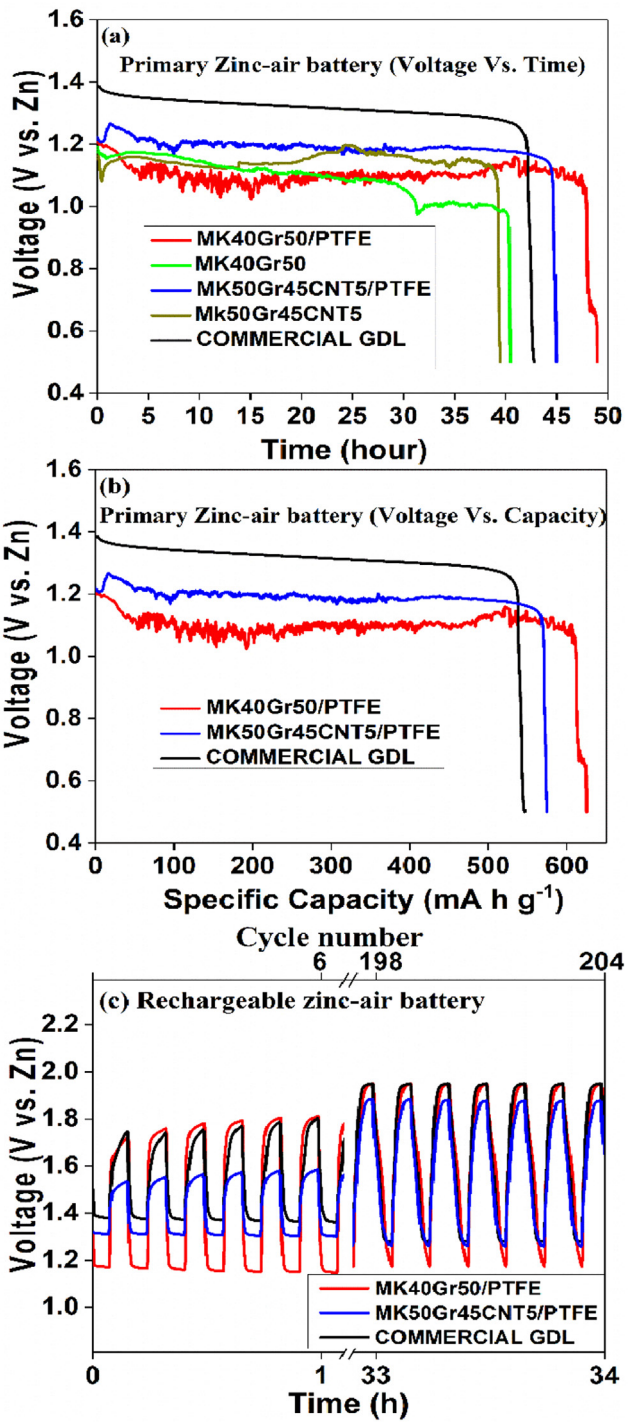

Fig. 7. Primary and secondary ZAB performance of ceramic GDLs at the current density of 3 mA/cm^2; (a) Complete discharge as a function of time, (b) Complete discharge as a function of specific capacity, (c) rechargeable performance. Commercial Pt-Ru/C was employed as catalyst and SIGRACET® 39 BC acted as reference GDL.

to the commercial electrode (specific capacitance: 542 mA h/g; discharge time: 43 h). It can be seen that the GDL coated with PTFE (MK40Gr50/PTFE, MK50Gr45CNT5/PTFE) show extended shelf life and breathe in even longer compared to its counterpart (MK40Gr50, MK50Gr45CNT5) since the superhydrophobic PTFE creates a better three-phase boundary region for improved ORR activity [37]. Overall, the ceramic GDLs, which have a sponge-like layer structure with aligned pores, high open porosity, and a

superior three-phase boundary region, potentially allow for more oxygen permeation and consequently facilitate the mass transport process [42].

Furthermore, galvanostatic discharge-charge measurements were conducted at a current density of 3 mA/cm^2, and round-trip efficiency was calculated after 200 cycles (Fig. 7c). The calculated round-trip efficiency of 60% and 67% is observed for MK40Gr50/PTFE and MK50Gr45CNT5/PTFE, respectively. When comparing with the commercial electrode (round-trip efficiency of 66%), it becomes evident that ceramic GDLs are a potential and efficient alternative for ZABs. Typical properties of ceramic GDLs, along with the ZAB performance, are summarized in Table 1. Finally, the morphological stability after the galvanostatic tests were investigated using SEM. Fig. 8 shows the top, bottom, and cross-sectional view of the MK50Gr45CNT5/PTFE based GDL after 200 cycles. It is worth noticing that no morphological change occurred after 200 cycles, as there is no significant difference to freshly prepared GDLs (Fig. 2) owing to the excellent mechanical stability and highly aligned porous bilayered geometry with a hydrophobic surface. While investigations of the as-prepared ceramic GDL on ZAB, the highly porous GDL (MK40Gr50) breathes even longer and delivers high capacity compared with low porous GDLs (MK50Gr50 and MK50Gr45CNT5). Whereas the highly conductive GDL (MK50Gr45CNT5) offers a slightly higher OCV and working potential. On the other hand, PTFE coated ceramic GDL such as MK40Gr50/PTFE and MK50Gr45CNT5/PTFE, promote better capacity, operating potential and reversibility, which are among the highest reported values so far. Hence as a combination of porosity, conductivity, and hydrophobicity appears as critical requirements for GDL, which improves the ZAB performance. Thus, this work demonstrates the benefits of using PDC shaped with freeze tape casting for the application as ceramic GDL in ZABs.

Table 1
Typical properties of ceramic gas-diffusion layer along with ZAB performance.

GDL*	Thickness (μm)	Open porosity (%)	Pores diameter (μm)	Hydrophobic behaviour (WCA) (°)	Electrical conductivity (S cm^{-1})	Tensile strength (MPa)	ZAB performance
MK40Gr50	400	55	5.6	120.2	1.89 * 10^{-4}	12.8	Specific capacity 625 mAh g^{-1}, 60% round-trif efficiency after 200 cycles
MK50Gr45CNT5	390	39	3.1	137.5	5.59 * 10^{-3}	24	Specific capacity 570 mAh g^{-1}, 67% round-trif efficiency after 200 cycles
CommercialGDL (SIGRACET® GDL 39 BC)	375	50	–	144.1	2 * 10^{-1}	–	Specific capacity 542 mAh g^{-1}, 66% round-trif efficiency after 200 cycles

* Pt-Ru/C as employed as cathode catalyst for ZAB testing.

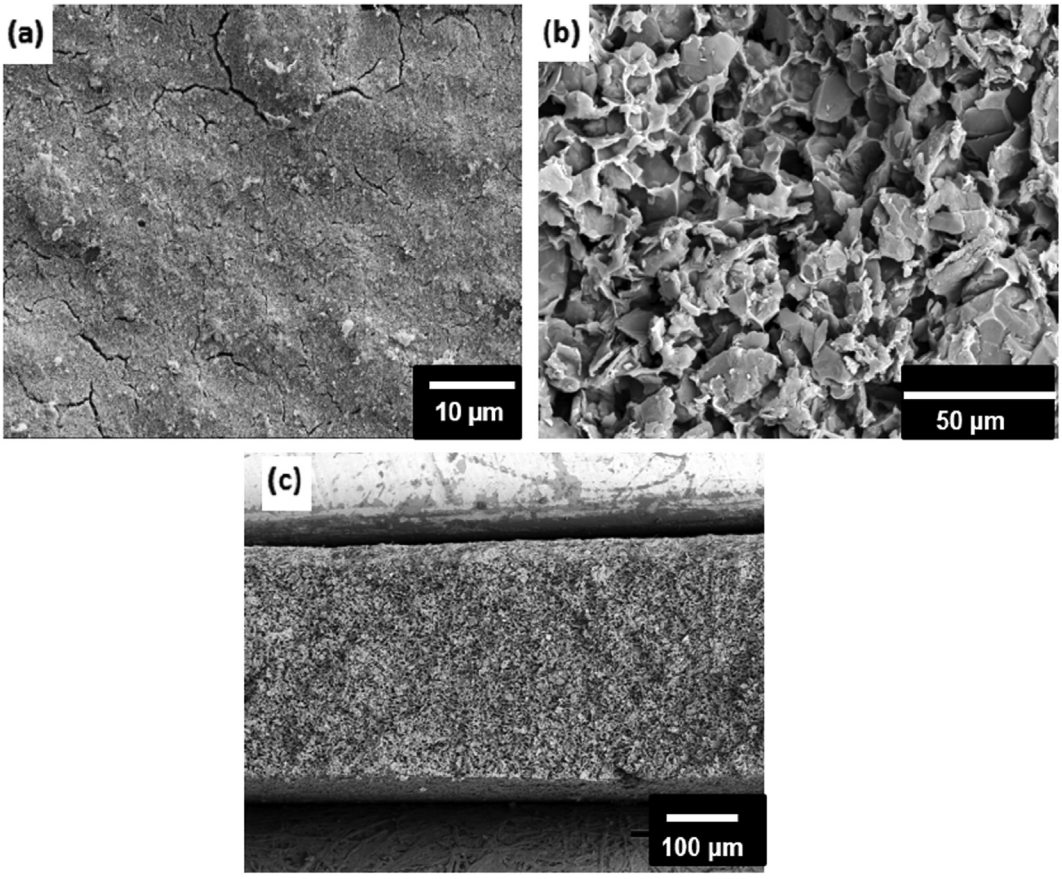

Fig. 8. SEM images of (a) top, (b) bottom and (c) cross-sectional view of cycled ceramic GDL made up of MK50Gr45CNT5/PTFE.

4. Conclusion

In summary, freeze tape casting techniques has been applied for the first time for the successful development of a new ceramic GDL for ZABs. The GDL showed non-aligned/aligned pores and an average pore diameter between 3 and 10 μm with open porosity of 55%. As expected, the PTFE coated GDL shows a hydrophobic behaviour with a better three-phase boundary region. The electrical conductivity of GDL has been increased five orders of magnitude with the addition of Gr/-CNT. Under ZAB working conditions, the ceramic electrode outperforms the commercial electrode with excellent capacity and cycling stability over 200 cycles, due to an improvement in the oxygen exchange rate and shorten pathways for oxygen ion/-electron kinetics as an effect of porosity, conductivity, and hydrophobicity. Finally, with the broad chemical variaty of PDCs and the excellent process control of freeze tape casting, this work sheds light on a new strategy to design 3D hierarchical porous ceramic GDL for next-generation energy ZAB.

CRediT authorship contribution statement

Prabu Moni: Conceptualization, Methodology, Investigation, Supervision, Writing - original draft. **Amanda Deschamps:** Investigation. **Daniel Schumacher:** Methodology, Writing - review & editing. **Kurosch Rezwan:** Writing - review & editing, Supervision. **Michaela Wilhelm:** Supervision, Project administration, Funding acquisition, Writing - review & editing.

Declaration of Competing Interest

The authors declare that they have no known competing financial interests or personal relationships that could have appeared to influence the work reported in this paper.

Acknowledgements

German Research Foundation (DFG) within the Brazilian-German Collaborative Research Initiative on Manufacturing (BRAGECRIM-WI 3131/5-1) supported this work. Additionally, DFG within the Research Training Group GRK 1860 “Micro-, meso- and macroporous nonmetallic Materials: Fundamentals and Applications” (MIMENIMA) is also gratefully acknowledged. Dr. Prabu Moni is grateful to the Department of Science and Technology (DST), New Delhi, India, for awarding the INSPIRE Faculty Award (DST/INSPIRE/04/2016/000530).

Appendix A. Supplementary data

Supplementary data to this article can be found online at https://doi.org/10.1016/j.jcis.2020.05.041.

References

[1] J. Fu, R. Liang, G. Liu, A. Yu, Z. Bai, L. Yang, Z. Chen, Recent progress in electrically rechargeable zinc-air batteries, Adv. Mater. 31 (31) (2019) e1805230.
[2] J. Pan, Y.Y. Xu, H. Yang, Z. Dong, H. Liu, B.Y. Xia, Advanced architectures and relatives of air electrodes in Zn-air batteries, Adv. Sci. (Weinh.) 5 (4) (2018) 1700691.
[3] J. Yi, P. Liang, X. Liu, K. Wu, Y. Liu, Y. Wang, Y. Xia, J. Zhang, Challenges, mitigation strategies and perspectives in development of zinc-electrode materials and fabrication for rechargeable zinc–air batteries, Energy Environ. Sci. 11 (11) (2018) 3075–3095.
[4] Z. Zhao, X. Fan, J. Ding, W. Hu, C. Zhong, J. Lu, Challenges in zinc electrodes for alkaline zinc-air batteries: obstacles to commercialization, ACS Energy Lett. 4 (9) (2019) 2259–2270.
[5] S.R. Dhanushkodi, F. Capitanio, T. Biggs, W. Mérida, Understanding flexural, mechanical and physico-chemical properties of gas diffusion layers for polymer membrane fuel cell and electrolyzer systems, Int. J. Hydrogen Energy 40 (46) (2015) 16846–16859.
[6] R. Omrani, B. Shabani, Gas diffusion layers in fuel cells and electrolysers: a novel semi-empirical model to predict electrical conductivity of sintered metal fibres, Energies 12 (5) (2019).
[7] A. Ozden, I.E. Alaefour, S. Shahgaldi, X. Li, C. Ozgur Colpan, F. Hamdullahpur, Gas diffusion layers for PEM fuel cells, exergetic, energetic and environmental, Dimensions (2018) 695–727.
[8] A. Jayakumar, S. Singamneni, M. Ramos, A.M. Al-Jumaily, S.S. Pethaiah, Manufacturing the gas diffusion layer for PEM fuel cell using a novel 3D printing technique and critical assessment of the challenges encountered, Materials (Basel) 10 (7) (2017).
[9] R. Schweiss, C. Meiser, T. Damjanovic, I. Galbiati, N. Haak, SIGRACET® Gas Diffusion Layers for PEM Fuel Cells, Electrolyzers and Batteries (White Paper), 2016.
[10] J. Pan, X.L. Tian, S. Zaman, Z. Dong, H. Liu, H.S. Park, B.Y. Xia, Recent progress on transition metal oxides as bifunctional catalysts for lithium-air and zinc-air batteries, Batteries Supercaps 2 (4) (2019) 336–347.
[11] F. Schulze-Küppers, U.V. Unije, H. Blank, M. Balaguer, S. Baumann, R. Mücke, W.A. Meulenberg, Comparison of freeze-dried and tape-cast support microstructure on high-flux oxygen transport membrane performance, J. Membr. Sci. 564 (2018) 218–226.
[12] Y. Xu, P. Deng, G. Chen, J. Chen, Y. Yan, K. Qi, H. Liu, B.Y. Xia, 2D nitrogen-doped carbon nanotubes/graphene hybrid as bifunctional oxygen electrocatalyst for long-life rechargeable Zn–air batteries, Adv. Funct. Mater. 30 (6) (2020) 1906081.
[13] P. Moni, W.F. Chaves, M. Wilhelm, K. Rezwan, Polysiloxane microspheres encapsulated in carbon allotropes: a promising material for supercapacitor and carbon dioxide capture, J. Colloid Interface Sci. 542 (2019) 91–101.
[14] P. Moni, M.G. Pollachini, M. Wilhelm, J. Lorenz, C. Harms, M.M. Murshed, K. Rezwan, Metal-containing ceramic composite with in situ grown carbon nanotube as a cathode catalyst for anion exchange membrane fuel cell and rechargeable zinc-air battery, ACS Appl. Energy Mater. 2 (8) (2019) 6078–6086.
[15] B.-B. Dong, F.-H. Wang, M.-Y. Yang, J.-L. Yu, L.-Y. Hao, X. Xu, G. Wang, S. Agathopoulos, Polymer-derived porous SiOC ceramic membranes for efficient oil-water separation and membrane distillation, J. Membr. Sci. 579 (2019) 111–119.
[16] Y. Feng, S. Lai, L. Yang, R. Riedel, Z. Yu, Polymer-derived porous Bi_2WO_6/SiC(O) ceramic nanocomposites with high photodegradation efficiency towards Rhodamine B, Ceram. Int. 44 (7) (2018) 8562–8569.
[17] D. Vrankovic, M. Graczyk-Zajac, C. Kalcher, J. Rohrer, M. Becker, C. Stabler, G. Trykowski, K. Albe, R. Riedel, Highly porous silicon embedded in a ceramic matrix: a stable high-capacity electrode for Li-ion batteries, ACS Nano 11 (11) (2017) 11409–11416.
[18] L. David, R. Bhandavat, U. Barrera, G. Singh, Silicon oxycarbide glass-graphene composite paper electrode for long-cycle lithium-ion batteries, Nat. Commun. 7 (1) (2016) 10998.
[19] T. Canuto de Almeida e Silva, V. Fernandes Kettermann, C. Pereira, M. Simões, M. Wilhelm, K. Rezwan, Novel tape-cast SiOC-based porous ceramic electrode materials for potential application in bioelectrochemical systems, J. Mater. Sci. 54 (8) (2019) 6471–6487.
[20] D. Hotza, R.K. Nishihora, R.A.F. Machado, P.M. Geffroy, T. Chartier, S. Bernard, Tape casting of preceramic polymers toward advanced ceramics: a review, Int. J. Ceram. Eng. Sci. 1 (1) (2019) 21–41.
[21] C. Gaudillere, J.M. Serra, Freeze-casting: Fabrication of highly porous and hierarchical ceramic supports for energy applications, Boletín de la Sociedad Española de Cerámica y Vidrio 55 (2) (2016) 45–54.
[22] H. Shen, E. Yi, M. Amores, L. Cheng, N. Tamura, D.Y. Parkinson, G. Chen, K. Chen, M. Doeff, Oriented porous LLZO 3D structures obtained by freeze casting for battery applications, J. Mater. Chem. A 7 (36) (2019) 20861–20870.
[23] H. Zhang, P. D'Angelo Nunes, M. Wilhelm, K. Rezwan, Hierarchically ordered micro/meso/macroporous polymer-derived ceramic monoliths fabricated by freeze-casting, J. Eur. Ceram. Soc. 36 (1) (2016) 51–58.
[24] D. Schumacher, P.H. da Rosa Braun, M. Wilhelm, K. Rezwan, Unidirectional solution-based freeze cast polymer-derived ceramics: influence of freezing conditions and templating solvent on capillary transport in isothermal wicking, J. Mater. Sci. (2019).
[25] Y. Chen, Y. Lin, Y. Zhang, S. Wang, D. Su, Z. Yang, M. Han, F. Chen, Low temperature solid oxide fuel cells with hierarchically porous cathode nanonetwork, Nano Energy 8 (2014) 25–33.
[26] Y. Hwa, E. Yi, H. Shen, Y. Sung, J. Kou, K. Chen, D.Y. Parkinson, M.M. Doeff, E.J. Cairns, Three-dimensionally aligned sulfur electrodes by directional freeze tape casting, Nano Lett. 19 (7) (2019) 4731–4737.
[27] S. Kokott, L. Heymann, G. Motz, Rheology and processability of multi-walled carbon nanotubes – ABSE polycarbosilazane composites, J. Eur. Ceram. Soc. 28 (5) (2008) 1015–1021.
[28] Y. Du, N. Hedayat, D. Panthi, H. Ilkhani, B.J. Emley, T. Woodson, Freeze-casting for the fabrication of solid oxide fuel cells: a review, Materialia 1 (2018) 198–210.
[29] D. Schumacher, M. Wilhelm, K. Rezwan, Modified solution based freeze casting process of polysiloxanes to adjust pore morphology and surface functions of SiOC monoliths, Mater. Des. 160 (2018) 1295–1304.
[30] D. Mackay, I. van Wesenbeeck, Correlation of chemical evaporation rate with vapor pressure, Environ. Sci. Technol. 48 (17) (2014) 10259–10263.

[31] P. Colombo, G. Mera, R. Riedel, G.D. Sorarù, Polymer-derived ceramics: 40 years of research and innovation in advanced ceramics, J. Am. Ceram. Soc. 93 (7) (2010) 1805–1837.
[32] M. Naviroj, P.W. Voorhees, K.T. Faber, Suspension- and solution-based freeze casting for porous ceramics, J. Mater. Res. 32 (17) (2017) 3372–3382.
[33] T. Liu, Y. Chen, S. Fang, L. Lei, Y. Wang, C. Ren, F. Chen, A dual-phase bilayer oxygen permeable membrane with hierarchically porous structure fabricated by freeze-drying tape-casting method, J. Membr. Sci. 520 (2016) 354–363.
[34] S. Deville, Freeze-casting of porous ceramics: a review of current achievements and issues, Adv. Eng. Mater. 10 (3) (2008) 155–169.
[35] K.L. Scotti, D.C. Dunand, Freeze casting – a review of processing, microstructure and properties via the open data repository, FreezeCasting. net, Prog. Mater. Sci. 94 (2018) 243–305.
[36] T. Canuto de Almeida e Silva, G.D. Bhowmick, M.M. Ghangrekar, M. Wilhelm, K. Rezwan, SiOC-based polymer derived-ceramic porous anodes for microbial fuel cells, Biochem. Eng. J. 148 (2019) 29–36.
[37] A. Flegler, S. Hartmann, J. Settelein, K. Mandel, G. Sextl, Screen printed bifunctional gas diffusion electrodes for aqueous metal-air batteries: combining the best of the catalyst and binder world, Electrochim. Acta 258 (2017) 495–503.
[38] R.K. Nishihora, E. Rudolph, M.G.N. Quadri, D. Hotza, K. Rezwan, M. Wilhelm, Asymmetric mullite membranes manufactured by phase-inversion tape casting from polymethylsiloxane and aluminum diacetate, J. Membr. Sci. 581 (2019) 421–429.
[39] J. Seuba, S. Deville, C. Guizard, A.J. Stevenson, Mechanical properties and failure behavior of unidirectional porous ceramics, Sci. Rep. 6 (2016) 24326.
[40] P. Moni, M. Wilhelm, K. Rezwan, The influence of carbon nanotubes and graphene oxide sheets on the morphology, porosity, surface characteristics and thermal and electrical properties of polysiloxane derived ceramics, RSC Adv. 7 (60) (2017) 37559–37567.
[41] E. Ionescu, A. Francis, R. Riedel, Dispersion assessment and studies on AC percolative conductivity in polymer-derived Si–C–N/CNT ceramic nanocomposites, J. Mater. Sci. 44 (8) (2009) 2055–2062.
[42] T. Danner, S. Eswara, V.P. Schulz, A. Latz, Characterization of gas diffusion electrodes for metal-air batteries, J. Power Sources 324 (2016) 646–656.